

REVIEW OF SYNCHROTRON RADIATION BASED DIAGNOSTICS FOR TRANSVERSE PROFILE MEASUREMENTS

G. Kube, DESY, Hamburg, Germany

Abstract

The transverse particle beam emittance is a crucial accelerator parameter because it is directly related to the brilliance of a synchrotron light source or the luminosity of a particle beam collider. Therefore a precise online control of the beam profile is highly desirable from which the corresponding emittance can be calculated. Due to its non-destructive nature synchrotron radiation from a bending magnet is a versatile tool for beam profile measurements and is used in nearly every accelerator. There exist a number of different techniques in order to overcome limitations due to resolution broadening effects which can result in theoretical resolutions down to the sub-micron level. In the present article an overview over the methods presently applied in most accelerators will be given, and examples for non-standard profile measurements like e.g. proton synchrotron monitors will be presented.

with a vertical opening angle of about $1/\gamma$. By choosing the radiation polarization the sensitivity of a profile monitor can be increased depending on the problem under investigation. The radiation properties can be calculated with high accuracy using e.g. numerical near field calculations [2] in order to study resolution broadening effects. Codes like SRW [3] or SPECTRA [4] are freely available allowing computations preserving all phase terms that are necessary for further propagation of the radiation through optical components. In SRW propagation is implemented in the frame of scalar diffraction theory applying the methods of Fourier optics. Finally the single particle radiation pulse is extremely short in the time domain and can even be modified by choosing the appropriate magnet structure which is of particular importance for proton SR diagnostics. All properties mentioned before are of importance for beam diagnostics and are reflected in the different monitor concepts.

INTRODUCTION

The production of low-emittance beams is one of the key techniques for electron accelerators and synchrotron light sources. A third-generation light source and future ones require emittances of a few nm rad and even less, and in high-energy physics the linear collider will have such an ultra-low emittance in order to realize the required luminosity. Not only production, also measurement and online control of a low emittance beam is a challenge because the beam profile to be resolved is in the order of a few tens of microns and even less. Therefore sophisticated schemes are necessary to measure the transverse beam emittance with sufficient accuracy, and there exist a number of different techniques in order to overcome limitations due to resolution broadening effects which can result in theoretical resolutions down to the sub-micron level.

Due to its non-destructive nature synchrotron radiation (SR) is a versatile tool for beam profile measurements and is used in nearly every accelerator. While in principle SR from insertion devices or bending magnets can be utilized, in reality most accelerators use bending magnet radiation based profile monitoring because of space limitations. Due to the relativistic energy of the particles the generated light has superior properties [1]:

The process of radiation generation is non-invasive and the radiation spectrum is continuous from infrared up to X-rays. As consequence the photon energy can be freely chosen according to the monitoring problem. Typically the spectrum is characterized by the critical energy $\hbar\omega_c = \frac{3}{2}\hbar c \frac{\gamma^3}{\rho}$ with γ the Lorentz factor and ρ the dipole bending radius. The natural divergence of the radiation is very small

PRINCIPLES

SR based transverse emittance diagnostics relies on the measurement of a photon spot size. While the emittance itself is no directly accessible value, beam size or beam divergence can be measured with a monitor system, thus leading to two different monitor concepts. With knowledge of the machine optical parameters, relative energy spread, monitor resolution and radiation properties the emittance can be extracted from the measured light spot. In the case of beam size measurements the simplest case is the direct imaging approach which is widely used for emittance diagnostics. The fundamental limit for such a measurement is given by Heisenberg's uncertainty relation which can be reformulated as $\Delta\sigma = \frac{\lambda}{2\Delta\Psi}$ in the specific case. Here $\Delta\sigma$ is the resolution broadening due to diffraction and $\Delta\Psi$ is the opening angle of the emitted photon. While the horizontal emission angle is large due to the particle motion on a curved trajectory in this plane in a bending magnet, the vertical one is small and thus imposing the fundamental resolution limit. For a typical optical wavelength of observation $\lambda = 500$ nm and an opening angle $\Delta\Psi = 1$ mrad, the resolution would amount $\Delta\sigma = 250$ μ m. Considering that the vertical beam size in a modern light source is in the order of a few tens of microns and even less, such a monitor would have a totally diffraction limited resolution. In order to overcome this limit there exist two different concepts. The most straightforward one is imaging at smaller wavelength in the VUV, soft or even hard X-ray region. In this case the discussion about a monitor concept is reduced to the question about the appropriate imaging optics. The second concept is an interferometric approach [5] which is

adapted from the stellar interferometer of Michelson used for the determination of the extent of stars [6]. It is based on the investigation of the spatial coherence properties of the radiation by measuring the blurring of the interferogram which depends on the particle beam size in a double-slit interferometric setup. The fundamental limit of this monitor principle is again Heisenberg's uncertainty relation which can be reformulated for an interferometric measurement as $\Delta n \Delta \Phi \sim 1$, with $\Delta \Phi$ the relative phase difference between the wave trains passing the two individual slits and Δn the number of required photons [7]. As consequence in order to measure the phase difference with high accuracy the intensity must be sufficient.

According to Ref. [8] the concepts for emittance monitoring can be classified in three categories, namely imaging, interference, and projection method. The principle for all methods is the same: the information about the beam spot is encoded onto a spatial resolving detector (CCD camera). The difference is in the way how the emitted wavefront is affected in between, and as consequence the signal from which the emittance will be deduced is either a beam spot, an interferogram, or an angular distribution.

In the following examples for these monitor concepts will be given with the emphasis on small beam size measurements, while a few examples for non-standard profile measurements will be shown at the end.

IMAGING METHODS

The most direct way for emittance diagnostics is the use of VUV or X-ray imaging techniques to obtain high quality radiation focusing, such that the spot size produced by a single particle is much smaller than the size of the beam as a whole (assuming 1:1 imaging). In this range of photon energies focusing optics can be realized either by reflection, diffraction, or refraction. All these principles are used in different emittance monitors and will be shortly described in the following. A comprehensive overview over X-ray focusing techniques can be found for example in Ref. [9].

Reflective Optics: External total reflection can occur when X-ray radiation hits a surface under grazing incidence. The critical angle of external total reflection θ_c can be calculated using Snell's law as $\theta_c = \sqrt{2\delta}$ with $\delta \approx 10^{-6}$ the refractive index decrement of the complex index of refraction. Due to the small angle of reflection in the order of $\theta \leq 0.5^\circ$ a simple spherical mirror would suffer from astigmatism. Thus the most common reflective optics is the Kirkpatrick-Baez setup [10] which consists of a pair of two consecutive cylindrical or elliptical mirrors. An example for a monitor system with such optics is the diagnostic beamline BL 3.1 of the ALS, Berkeley [11]. In this setup the beam spot is imaged onto a scintillator converting the broad X-ray spectrum into a visible image that is viewed by a microscope connected to a video camera. A carbon filter is used to remove synchrotron light with wavelengths longer than 10 nm for to reduce diffraction effects.

Diffraction Optics: The Fresnel zone plate (FZP) has become the most important diffractive optics in X-ray physics, and in the soft X-ray range of the electromagnetic spectrum it is still the best device for microanalysis. The zone plate consists of concentric rings, alternatingly transparent and opaque. The spacing of the rings is chosen such that the penetrating light waves interfere constructively at the focal point, i.e. the parts of the wave front which contribute with opposite sign in phase are absorbed. The width of the outermost zone Δr defines the zone plate resolution $\delta \approx 1.22 \times \Delta r$ and their focal length $f = \frac{4N(\Delta r)^2}{\lambda}$, N is the number of zones and λ the observation wavelength [12]. The latter condition shows that zone plate imaging requires a monochromator because of strong chromatic aberrations.

An example for a beam size monitor using a single zone plate is the X-ray beam imager at SPring-8 [13, 14]. It requires a diagnostic beamline of about 41 m. SR of 8.2 keV from a bending magnet is selected via the (111) reflection of a silicon double crystal monochromator and imaged by the zone plate onto a commercial X-ray zooming tube. The total magnification of the system is 13.7, the spatial resolution 4.1 μm .

The FZP monitor at ATF (KEK) is based on X-ray imaging optics with two FZPs and has the structure of a long-distance microscope [15, 16]. The radiation monochromatization at an energy 3.235 keV is achieved via the (220) reflection of a silicon single crystal monochromator. The 20 times magnified beam image is recorded via a direct incidence, back-thinned illuminated X-ray CCD, thus avoiding resolution broadening in the conversion from X-rays to visible light via a scintillator. The total spatial resolution of this monitor is estimated to 0.7 μm (rms). Using a fast mechanical shutter with opening shutter times ≤ 1 msec it was possible to resolve a vertical beam size of 6.4 μm by removing the effect of an unknown 100 Hz beam oscillation which blurred the vertical size.

A diffractive optics similar to the FZP is the Bragg-Fresnel lens used at ESRF [17] resp. the Bragg-Fresnel multilayer still in use at BESSY-II [18].

Refractive Optics: Refractive X-ray lenses have been considered for a long time as not feasible due to the weak refraction and the relatively strong absorption of X-rays in matter. While the first lenses were fabricated by drilling well aligned holes in aluminium, in the meantime it is possible to produce lenses with rotationally parabolic profile even from beryllium [19]. For a focusing surface this is the optimal shape because it modifies the quadratic terms of the radiation phase essential for focusing without introducing extra aberrations [8]. In order to keep the focal length f at reasonable values N individual lenses are stacked behind each other, resulting in $f = \frac{R}{2N\delta}$ (in thin lens approximation) with the refractive index decrement $\delta \approx 10^{-6}$ and the surface radius of curvature $R \approx 200 \mu\text{m}$ [20, 21]. Because of the large number of lenses ($N = 10 \dots 300$) these devices are called compound refractive lenses (CRLs). Due to the strong dependence of the refractive index decrement

on the photon energy a CRL based profile monitor requires also the use of a monochromator.

So far only one experiment for electron beam imaging using a single refractive lens is published from ESRF [22]. For the new high-brilliance synchrotron light source PETRA III at DESY it is planned to built up a CRL based emittance monitor with 31 beryllium lenses at a photon energy of 20 keV with an estimated monitor resolution of about 1 μm .

Focus-Free (Pinhole) Imaging: While the imaging principles described so far are based on focusing optics, the pinhole optics - without any focusing of the rays at all - is by far the least complicated device. The principle was already known to Aristoteles (384-322 b.C.) and described in his opus "Problemata". The X-ray pinhole camera has the advantage of a simple setup, it is used typically without monochromator and sometimes even outside the vacuum system, is insensitive to heat load, and has a high practical reliability. The drawback of a pinhole based emittance monitor is the limited resolution of $\geq 10 \mu\text{m}$.

Pinhole setups are the most common emittance monitors because of the well proven techniques and are used in a widespread number of accelerators as for example at ESRF [23], APS (Argonne) [24], SLS (PSI) [25], and even at the new third generation light sources just put to operation like DIAMOND [26] and SOLEIL [27] and planned ones like ALBA [28] and PETRA III.

The extension of the conventional pinhole monitor with only one aperture is the pinhole array which allows the simultaneous measurement of beam size and vertical beam divergence. Pinhole array monitors are used in the meantime at BESSY II [18], at ALS [29], and at the Australian Light Source [30].

Exploitation of Wave-Optics Features: According to Ref. [8] the use of small radiation wavelengths is not the only approach to improve the resolution for beam size measurements. Another possibility is the exploitation of the wave-optics features of SR, as for example imaging with visible light using the vertical (π) polarization component. The underlying principle is to make use of the on-axis minimum of the π polarized vertical intensity distribution which will be blurred with increasing vertical beam size. From the measured peak-to-valley ratio of the imaged beam spot it is therefore possible to extract the vertical size. This mechanism was applied for the first time at MAX-II [31] and is now used at SLS (PSI), showing good agreement with independent pinhole measurements [25].

INTERFERENCE METHODS

The principle of the interferometric method is based on the investigation of the spatial coherence of SR. In order to quantify the coherence properties usually the first order degree of mutual spatial coherence $\gamma(D)$ is used (c.f. for example Ref. [32]) with D the distance between two

wave-front dividing slits, see Fig. 1. The interferometer itself is a wave-front-division-type two-beam interferometer which uses polarized quasimonochromatic radiation. The intensity of the interference pattern measured in the detector plane directly depends on γ [5]:

$$I(y_0) = I_0 \left[\text{sinc}\left(\frac{2\pi a}{\lambda_0 R}\right) \right]^2 \left[1 + |\gamma| \cos\left(\frac{2\pi D}{\lambda_0 R} + \varphi\right) \right] \quad (1)$$

with a the half of the single slit height and D, R as indicated in Fig. 1, λ_0 the wavelength of observation and I_0 the sum of the incoherent intensities from both slits. Under condition of Fraunhofer diffraction (i.e. in far-field limit) the van Cittert-Zernicke theorem [32] relates the degree of coherence γ with the normalized source distribution $f(y)$:

$$\gamma(\nu) = \int dy f(y) \exp(-i2\pi\nu y), \quad (2)$$

where $\nu = \frac{D}{\lambda_0 R_0}$ denotes the spatial frequency.

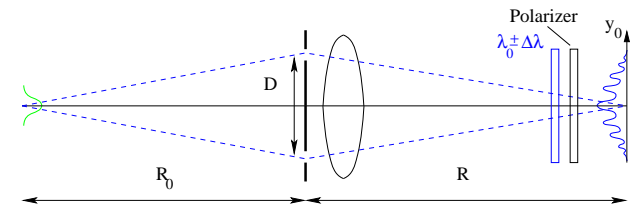


Figure 1: Principle setup for interferometric beam size measurements.

There are two operational modes for the interferometer: in the scanning mode the intensity pattern is recorded for varying slit distance D . From a fit to each individual interferogram Eq.(1) the functional dependency of $\gamma(D)$ can be determined and the beam shape $f(y)$ can be reconstructed by evaluating the Fourier back transform from Eq.(2). If the beam shape $f(y)$ is known to be normal distributed with width σ_y a single measurement for fixed slit distance D_0 is sufficient in order to determine σ_y from the relation

$$\sigma_y = \frac{\lambda_0 R_0}{\pi D_0} \sqrt{\frac{1}{2} \ln \frac{1}{\gamma(D_0)}}, \quad (3)$$

while $\gamma(D_0)$ has to be fitted again from the recorded interferogram. The latter mode of operation for fixed slit distance was applied in most interferometric applications. A comprehensive overview concerning the development of the SR interferometer can be found in Ref. [33]

SR interferometers are in use at a widespread number of accelerators as for example the KEK-ATF damping ring [34], ELETTRA [35], and PEP-II [36]. At SPring-8 even a two-dimensional interferometer was realized [37].

As mentioned before the interferometer relies on a precise phase measurement with the prerequisite of sufficient intensity. In order to fulfill this condition at KEK-ATF a 400 nm bandpass filter with large bandwidth of 80 nm was used. It could be demonstrated that for this setup the dominant error results from the dispersion in the refractive optics (lenses), leading to a blurring of the interferogram and

therefore reduced accuracy. As consequence the interferometer was recently improved by using reflective Herschelian optics [38]. With this setup a vertical beam size of $4.73 \mu\text{m}$ could be resolved while the beam size measured under same conditions with refractive optics amounted $7.2 \mu\text{m}$.

PROJECTION METHODS

Projection methods in context with SR from bending magnets for emittance diagnostics are not very common and used mainly at ESRF [39] and ANKA [40]. Due to the horizontal fan from bending magnet radiation only the vertical emittance can be determined.

The principle of this method relies on the fact that only a tiny fraction of very hard X-rays can fully penetrate the dipole crotch absorber and enter in the free air space behind. These X-rays with energies $\geq 70 \text{ keV}$ at ANKA resp. $\geq 150 \text{ keV}$ at ESRF are detected by a simple, compact and low-cost device consisting of a CdWO_4 scintillator and a standard CCD camera system.

With knowledge of the measured photon spot size $\sigma_{\gamma,y}$, the mean square photon emission angle $\langle \vartheta_{\gamma}^2 \rangle$, the distance between source and image plane L , and the accelerator Twiss parameters at the emission point the emittance can be derived in a similar way to the formalism developed in Ref. [23] as

$$\varepsilon_y = \frac{\sigma_{\gamma,y}^2 - \langle \vartheta_{\gamma}^2 \rangle L^2}{\beta_y + 2\alpha_y L + \gamma_y L^2}. \quad (4)$$

At the ep-collider HERA at DESY the projection method was used mainly for control of the electron beam position and slope at the interaction points of the colliding beam experiments ZEUS and H1. Nevertheless from the measured beam spot also an estimate for the vertical emittance could be derived which was in fair agreement with different on-line emittance measurements.

NON-STANDARD MEASUREMENTS

In case of proton accelerators the critical wavelength characterizing the SR emission spectrum from a bending magnet is shifted towards the infrared or even millimeter region because of the large proton rest mass. Optical elements are not easily available in these spectral regions and the image resolution would be deteriorated due to an increased contribution from diffraction broadening. In order to overcome these limitations the SR emission spectrum can be extended to higher frequencies if radiation produced in dipole fringe fields or in short magnets is used which contains sufficient intensity to render possible beam profile measurements. In order to understand the increase of intensity at higher frequencies it is helpful to recall the SR field properties in time domain (see for example Ref. [1]) because both quantities are simply related by the square of the absolute value of the Fourier transform.

The typical SR frequency is determined by the length of the radiation pulse seen by an observer. While the dura-

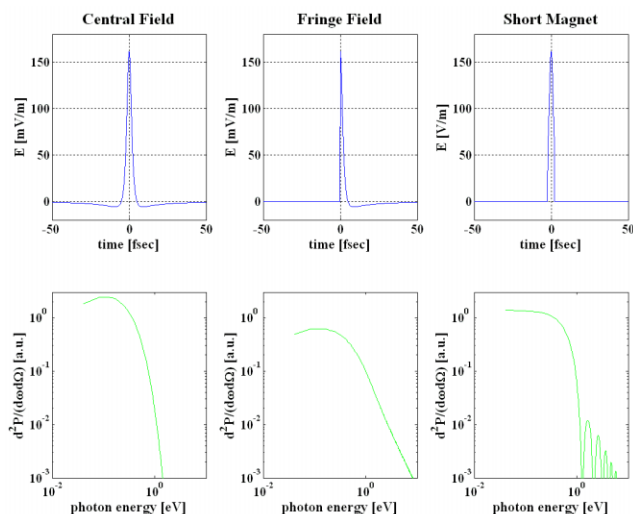


Figure 2: Time dependence of SR electrical field (top) and spectral power (bottom) for central field region (left), fringe field (center), and short magnet (right).

tion of the SR electric field produced in the central part of a bending magnet from a 6 GeV electron is in the order of 10^{-2} asec, for a 920 GeV proton it is in the order of fsec (see Fig. 2 left). In order to increase the intensity at higher frequencies a sharp cut-off of the wave train in time domain is necessary as it can be realized by a magnetic fringe field (Fig. 2 center) or a short magnet (Fig. 2 right).

While the SR intensity strongly depends on the proton energy the application of proton beam diagnostics is restricted to only a few accelerators. The first profile monitor based on this principle was realized at the SPS (CERN) [41]. The fringe field between two successive dipole magnets was used for radiation generation. While this monitor worked only at energies above about 350 GeV it was replaced later by an undulator which extended the usable energy range [42]. A similar beam profile monitor has been installed at Tevatron (FNAL) where synchrotron light produced from protons (antiprotons) at the upstream edge of a superconducting magnet is observed [43]. At HERA (DESY) the fringe field of a normal conducting vertical deflecting bending magnet was used to measure the beam size and to perform dynamical studies [44]. For the LHC it is also planned to use this type of monitor for transverse beam diagnostics. In order to optimize the performance over the whole energy range from 450 GeV up to 7 TeV, a superconducting undulator together with a separation dipole will act as radiation source [45].

SR based diagnostics is even not restricted to circular accelerators: at the ESRF the injector complex including two transfer lines utilizes SR profile monitors [46], and in the first bunch compressor of the VUV-FEL FLASH at DESY profile measurements are used to gain information about the energy distribution in a bunch due to the strong dispersion [47].

SUMMARY

This article comprises various techniques presently used mainly at synchrotron light sources for small emittance and profile measurements. Moreover the principles of SR based diagnostics for proton accelerators are summarized and it was shown that the application of SR monitoring is not restricted to circular accelerators.

In addition to emittance diagnostics manifold problems in accelerator physics can be studied with a SR profile monitor. From the huge number of applications only a few will be mentioned as examples: injection mismatch studies [48], turn-by-turn imaging [49], beam halo studies [50], and beam-beam induced beta beating measurements [51].

REFERENCES

- [1] A. Hofmann, *The Physics of Synchrotron Radiation*, Cambridge University Press, Cambridge 2004.
- [2] O. Chubar, *Rev. Sci. Instrum.* **66** (1995), 1872.
- [3] O. Chubar and P. Elleaume, *Proceedings of the EPAC'98*, Stockholm, Sweden (1998), 1177.
- [4] T. Tanaka and H. Kitamura, *J. Synchrotron Rad.* **8** (2001), 1221.
- [5] T. Mitsuhashi, *Proc. of the Joint US-CERN-Japan-Russia School on Particle Accelerators*, Montreux, 11-20 May 1998, (World Scientific), pp. 399-427.
- [6] A.A. Michelson, *Astrophys. J.* **51** (1920), 257.
- [7] S.G. Lipson, H.S. Lipson, D.S. Tannhauser, *Optical Physics*, Cambridge University Press, Cambridge 1995.
- [8] O. Chubar, *Proceedings of the EPAC'00*, Vienna, Austria (2000), 117.
- [9] I. Snigireva and A. Snigirev, *J. Environ. Monit.* **8** (2006), 33.
- [10] P. Kirkpatrick and A.V. Baez, *J. Opt. Soc. Am.* **38** (1948), 766.
- [11] T.R. Renner, H.A. Padmore, and R. Keller, *Rev. Sci. Instrum.* **67** (1996), 3368.
- [12] D.T. Attwood, *Soft X-rays and extreme ultraviolet radiation principles and applications*, Cambridge University Press, Cambridge 2000.
- [13] S. Takano, M. Masaki, and H. Ohkuma, *Proc. DIPAC'05*, Lyon, France (2005), 241.
- [14] S. Takano, M. Masaki, and H. Ohkuma, *Nucl. Instrum. Meth. A* **556**, (2006), 357.
- [15] H. Sakai et al., *Proc. EPAC'06*, Edinburgh, Scotland (2006), 2784.
- [16] H. Sakai et al., *Phys. Rev. ST Accel. Beams* **10** (2007), 042801.
- [17] Ya. Hartmann et al., *Rev. Sci. Instrum.* **66** (1995), 1978.
- [18] K. Holldack, J. Feikes, and W.B. Peatman, *Nucl. Instrum. Meth. A* **467-468**, (2001), 235.
- [19] C.G. Schroer et al., *Design and Microfabrication of Novel X-Ray Optics*, ed. D.C. Mancini (Bellingham, WA:SPIE), *Proc. SPIE* **4783** (2002), 10.
- [20] B. Lengeler et al., *J. Synchrotron Rad.* **6** (1999), 1153.
- [21] B. Lengeler et al., *J. Phys. D: Applied Phys.* **38** (2005), A218.
- [22] T. Weitkamp et al., *Proceedings of the EPAC'00*, Vienna, Austria (2000), 1824.
- [23] P. Elleaume et al., *J. Synchrotron Rad.* **2** (1995), 209.
- [24] M. Borland et al., *Proceedings of the EPAC'98*, Stockholm, Sweden (1998), 1556.
- [25] Å. Andersson et al., *Proceedings of the EPAC'06*, Edinburgh, Scotland (2006), 1223.
- [26] C.A. Thomas and G. Rehm, *Proc. DIPAC'05*, Lyon, France (2005), 93.
- [27] J.C. Denard et al., *Proc. DIPAC'03*, Mainz, Germany (2003), 6.
- [28] U. Irso and F. Pérez, *Proceedings of the EPAC'06*, Edinburgh, Scotland (2006), 3410.
- [29] F. Sannibale et al., *Proceedings of the EPAC'04*, Lucerne, Switzerland (2004), 2783.
- [30] M.J. Boland et al., *Proceedings of the EPAC'06*, Edinburgh, Scotland (2006), 3263.
- [31] Å. Andersson, *Electron beam profile measurements and emittance manipulation at the MAX-laboratory*, Ph.D. thesis, Lund 1997.
- [32] M. Born and E. Wolf, *Principles of Optics*, Pergamon Press Ltd., New York, 1980.
- [33] T. Mitsuhashi, *Proc. of BIW'04*, Knoxville, Tennessee, AIP Conf. Proceedings **732** (2004), 3.
- [34] H. Hayano et al., *Proc. of the PAC'99*, New York (1999), 2143.
- [35] F. Iazzourene et al., *Proceedings of the EPAC'00*, Vienna, Austria (2000), 1732.
- [36] A.S. Fisher et al., *Proc. of the PAC'01*, Chicago (2001), 547.
- [37] M. Masaki and S. Takano, *J. Synchrotron Rad.* **10** (2003), 295.
- [38] T. Naito and T. Mitsuhashi, *Phys. Rev. ST Accel. Beams* **9** (2006), 122802.
- [39] K. Scheidt, *Proc. of BIW'06*, Batavia, Illinois, AIP Conf. Proceedings **868** (2006), 208.
- [40] A.S. Muller et al., *Proceedings of the EPAC'06*, Edinburgh, Scotland (2006), 1073.
- [41] R. Bossart et al., *Nucl. Instrum. Meth.* **164** (1979), 375.
- [42] J. Bossert et al., CERN-SPS/83-5 (1983).
- [43] R. Thurman-Keup, *Proc. of BIW'06*, Batavia, Illinois, AIP Conf. Proceedings **868** (2006), 364.
- [44] G. Kube et al., *Proc. of BIW'06*, Batavia, Illinois, AIP Conf. Proceedings **868** (2006), 374.
- [45] L. Ponce, R. Jung, F. Méot, CERN-2004-07 (2004).
- [46] K. Scheidt, *Proc. DIPAC'05*, Lyon, France (2005), 24.
- [47] Ch. Gerth, these proceedings.
- [48] M.G. Minty and W.L. Spencer, *Proc. of the PAC'95*, Dallas (1995), 536.
- [49] O.I. Meshkov et al., *Proc. DIPAC'05*, Lyon, France (2005), 42.
- [50] T. Mitsuhashi, *Proc. DIPAC'05*, Lyon, France (2005), 7.
- [51] G. Kube and F. Willeke, *Proceedings of the EPAC'06*, Edinburgh, Scotland (2006), 1046.